High-performance liquid chromatography separation of unsaturated organic compounds by a monolithic silica column embedded with silver nanoparticles.

AUTHOR(S):

Zhu, Yang; Morisato, Kei; Hasegawa, George; Moitra, Nirmalya; Kiyomura, Tsutomu; Kurata, Hiroki; Kanamori, Kazuyoshi; Nakanishi, Kazuki

CITATION:

Zhu, Yang ...[et al]. High-performance liquid chromatography separation of unsaturated organic compounds by a monolithic silica column embedded with silver nanoparticles.. Journal of separation science 2015, 38(16): 2841-2847

ISSUE DATE:

2015-08

URL:

http://hdl.handle.net/2433/202103

HPLC Separation of Unsaturated Organic Compounds by Ag Nanoparticles Embedded Monolithic Silica Column

Yang Zhu[1], Kei Morisato[2], George Hasegawa[1], Nirmalya Moitra[1], Tsutomu Kiyomura[3], Hiroki Kurata[3], Kazuyoshi Kanamori[1], Kazuki Nakanishi[1]

[1] Department of Chemistry, Graduate School of Science, Kyoto University, Kitashirakawa, Sakyo-ku, Kyoto 606-8502, Japan

[2] GL Science, Inc. 237-2 Sayamagahara, Iruma, Saitama, 358-0032, Japan

[3] Institute for Chemical Research, Kyoto University, Uji, 611-0011, Japan

Correspondence: Associate Professor Kazuki Nakanishi, Department of Chemistry, Graduate School of Science, Kyoto University, Kitashirakwa, Sakyo-ku, Kyoto 606-8502, Japan

E-mail: kazuki@kuchem.kyoto-u.ac.jp

FAX: +81 75 753 2925

Abbreviations: NPs, nanoparticles; PAHs, polyaromatic hydrocarbons; RP, reversed phase; PMSM, periodic mesoporous silica monolith; TEOS, tetramethoxysilane; PEO, poly(ethylene oxide); APTES, (3-aminopropyl)triethoxysilane; SEM, scanning electron microscopy; FE-SEM, field emission scanning electron microscopy; TEM, transmittance electron microscopy; XRD, X-ray diffraction; TG-DTA, thermogravimetry-differential thermal analysis; FT-IR, Fourier transform infrared spectroscopy; XPS, X-ray photoelectron spectroscopy; h, reduced plate height.

Key words: Ag nanoparticles, *Cis/trans* isomers, High-performance liquid chromatography, Monolithic silica column, Polyaromatic hydrocarbons

Abstract

The optimization of porous structure which ensures good separation performances is always a significant issue in HPLC column design. Recently we reported the homogeneous embedment of Ag nanoparticles in periodic mesoporous silica monolith and the application of such Ag nanoparticles embedded silica monolith for HPLC separation of polyaromatic hydrocarbons. However, the separation performance remains to be improved and the retention mechanism as compared with Ag ion HPLC technique, still needs to be clarified. In this research, Ag nanoparticles were introduced into a macro/mesoporous silica monolith with optimized pore parameters for HPLC separations. Baseline separation of benzene, naphthalene, anthracene and pyrene was achieved with the theoretical plate number for analyte naphthalene as 36000 m^{-1}. Its separation function was further extended to *cis/trans* isomers of aromatic compounds where *cis/trans* stilbenes were chosen as a benchmark. Good separation of *cis/trans* stilbene with separation factor as 7 and theoretical plate number as 76000 m^{-1} for *cis*-stilbene was obtained. The *trans* isomer, however retains stronger which contradicts the long established retention rule of Ag ion chromatography. Such behavior of Ag nanoparticles embedded silica column can be attributed to the differences in the molecular geometric configuration of *cis/trans* stilbenes.

1 Introduction

Applicability of so-called nanomaterials in separation science has been proven and demonstrated for these decades. Silica nanoparticles (NPs) are the first nanomaterial to be utilized either as the stationary phase or a modifier supported by silica or other matrices for chromatography techniques [1-4]. In recent years, other inorganic nanomaterials (zirconia, titania, alumina, iron oxide, hydroxyapatite, carbon-based material) and some polymer nanobeads supported by silica or polymeric stationary phase were also applied to different chromatography techniques including gas chromatography [5,6], capillary liquid chromatography [7-11] and capillary electrochromatography [12-14].

Noble metal NPs, as an extended important category among all the nanomaterials, have found their applications in different fields. Among them, gold NPs, due to its well-known affinity towards amino- and thiol-containing molecules, were immobilized on stationary phase and used for chromatographic separations. Yang et al. embedded gold NPs in a fused-silica capillary column and achieved efficient separation of polyaromatic hydrocarbons (PAHs) under an open-tubular CEC condition [15]. Recently Svec et al. attached gold NPs on porous polymer monoliths in a capillary and carried out the separation of molecules such as cysteine-containing peptides in acetonitrile or water as the mobile phase [16] and nucleosides under the HILIC mode [17]. Meanwhile, Liang et al. immobilized gold NPs on a graphene oxide/silica composite stationary phase and demonstrated the separation of alkylbenzenes, benzenediol isomerides, amino acids, nucleosides and nucleobases in both reversed-phase (RP) mode and HILIC mode with good separation performance [18]. Each aforementioned research showed high potential of gold NPs for chromatographic separations of different molecules under different conditions.

Separation of lipids by silver ion chromatography has been scientifically studied and industrially applied for decades [19,20]. Only a limited number of researches, however, have been reported on the application of metallic Ag NPs for separations [21]. Recently we, for the first time, reported a method of homogeneous immobilization of Ag NPs in a macroporous silica monolith embedded with SBA-15 type periodic mesopores

(denoted as periodic mesoporous silica monolith: PMSM), which was further used for HPLC separation of PAHs. Similar retention characteristics for unsaturated compounds were shown as compared with silver ion chromatography [20,22]. Nevertheless, the separation performance was relatively poor (no baseline separation for benzene, naphthalene and anthracene when injected together and separation factor 0.43 for anthracene) even though the Ag loading in PMSM was relatively high (32 mg per column). The inadequacy of separation efficiency is mainly attributed to characteristic pore structure of the host silica, undesirable for HPLC separation. On the macropore scale, the pressure-driven liquid flow through polygonal-shaped macroporous channels of PMSM potentially generates a more inhomogeneous flow profile compared to the Poiseuille-type one, which is undesirable for high efficiency separations [23]. Meanwhile on the mesopore scale, relatively small-sized mesopores (average 9 nm) become even smaller (average 7 nm) after the embedment of Ag NPs, which limits the accessibility of analyte molecules to the NPs.

In this research, aiming at improved separation performance of Ag NPs/silica HPLC columns, a silica column with improved porous structure for HPLC separation was chosen as a host. After the introduction of Ag NPs, the resultant monolith has been made into a HPLC column and subjected to the separation of PAHs as well as *cis*/*trans* stilbene isomers. Good baseline separation for both PAHs and *cis*/*trans* stilbene isomers were achieved with the theoretical plate number reaching 76000 m^{-1} for the analyte *cis* stilbene and the separation factor as high as 7 for *cis*/*trans* stilbene isomers. The better separation performance with less Ag loading (25 mg per column) was explained by the synergic effect from host silica monolith with optimized porous structure. An opposite result of the elution order of *cis* and *trans* stilbenes as compared with that of silver ion chromatography was observed in Ag NPs embedded silica column. Such phenomenon is mainly resulted from the more planar molecular geometry of *trans* stilbene than its *cis* isomer.

2 Materials and Methods

2.1 Materials

As the silica source, tetramethoxysilane (TMOS) was purchased from Shin-Etsu Chemical Co. Ltd. (Japan). Poly(ethylene oxide) (PEO, *M*w = 10000) as the phase separation inducer for the preparation of monolithic

silica, (3-aminopropyl)triethoxysilane (APTES), silver nitrate, naphthalene, anthracene, phenanthrene, *cis*-stilbene and *trans*-stilbene were obtained from Sigma-Aldrich Co. LLC (USA). Urea and distilled water were purchased from Hayashi Pure Chemical Ind., Ltd. (Japan) and Wako Pure Chemical Ltd. (Japan), respectively. All the other chemicals were from Kishida Chemical Co., Ltd. (Japan). All the chemicals were of analytical grade and used without further purification.

2.2 Preparation of monolithic silica gel and Ag NPs embedded silica gel

Monolithic silica bearing continuous macropores and size-expanded mesopores was prepared by our previously reported procedure [24]. The introduction of Ag NPs homogeneously into monolithic silica follows the method reported in one of our recent literatures with some modifications [22]. In a typical run, 0.60 g of silica monolith was immersed into 20 mL of 170 mM APTES/toluene solution in a sealed amber tube and left for reaction at 80 °C for 24 h for the modification of silica surface with aminopropyl groups. The modified monolith was later washed with excess amount of ethanol at 50 °C. The obtained monolith was then immersed in 20 mL of 50 mM $AgNO_3$/ethanol solution at room temperature for the immobilization of Ag ion on aminopropyl groups and in-situ reduction by ethanol, which acts both as the solvent and the reductant. Since the silica monolith used in the present study has higher density than the one used in the previous study, in order to achieve higher loading of Ag NPs, the reaction time of $AgNO_3$ solution with the aminopropyl-modified silica was elongated to 14 d, as compared with 4 d in the previous report. The color of the monolith turned from white to black due to the immobilization of Ag NPs on the skeleton surface. The resultant monolith was then washed with sufficient amount of ethanol and the total removal of Ag ion in the monolith was confirmed by the absence of formation of AgCl precipitate after adding 0.1 M HCl aqueous solution into the ethanol obtained after washing for several times. The monolith was then dried at 60 °C for more than 3 days and was denoted as SiO_2-NH_2-Ag. As a comparison, pure silica monolith and silica monolith modified with aminopropyl groups were synthesized as well and denoted as SiO_2 and SiO_2-NH_2, respectively and those derivatives of PMSM were denoted as PMSM-NH_2, PMSM-NH_2-Ag, among which, the Ag loading in PMSM-NH_2-Ag was reached by repeated treatment for 3 times [22].

2.3 Characterizations

Macroscopic and mesoscopic morphologies of the monolithic samples were confirmed by scanning electron microscopy (SEM, JSM-6060S, JEOL, Japan) and field emission scanning electron microscopy (FE-SEM, JSM-6700F, JEOL, Japan). Meso- and microstructure of the samples were characterized by nitrogen adsorption-desorption (BELSORP-mini II, Bel Japan Inc., Japan). The size and morphology of Ag NPs embedded in the silica monolith were investigated by transmittance electron microscopy (TEM, JEM-2200FS, JEOL, Japan) equipped with a spherical aberration corrector (CETCOR, CEOS GmbH, Germany). The crystal structure was confirmed by powder X-ray diffraction (XRD, RINT Ultima III, Rigaku Co., Japan) using Cu Kα (λ = 0.154 nm) as an incident beam. Thermal properties of the samples were investigated by thermogravimetry-differential thermal analysis (TG-DTA, Thermo plus TG 8120, Rigaku Co., Japan) with a continuous air supply at 100 mL/min. Fourier transform infrared spectroscopy (FT-IR, IR Affinity-1, Shimadzu Co., Japan) and X-ray photoelectron spectroscopy (XPS, MT-5500, ULVAC-PHI Inc. Japan) were performed to confirm the molecular and atomic level information. Since nitric acid was formed as a side product and most of it further reacted with aminopropyl groups on the silica surface via acid-base reaction to form $-NH_3^+NO_3^-$ ion pairs [21], the Ag loading in the monolith was calculated from the weight of reacted $AgNO_3$ by weighing the dried samples before and after the reduction process.

2.4 Chromatographic measurements

Liquid chromatographic evaluations were carried out using an ordinary HPLC system with a pump (PU712, GL Sciences, Japan), a UV detector (MU701, GL Sciences, Japan), a data processor (EZ Chrom Elite Chromatography Data System, Agilent Technologies, USA), and a Rheodyne injector (8125, Rheodyne, USA). The system was operated in an isocratic mode at room temperature (~ 25 °C). For the separation of PAHs, 1.6 µL of benzene, 0.8 mg of naphthalene, 0.2 mg of anthracene, and 0.5 mg of phenanthrene were dissolved separately in 1 mL of *n*-hexane as the standard samples for columns made from SiO_2 and SiO_2-NH_2 monoliths. For columns made from SiO_2-NH_2-Ag monolith, all the compounds were dissolved together in *n*-hexane. The injection volume was 1 µL in each case.

3 Results and Discussion

3.1 Synthesis of Ag NPs embedded silica monolith

Co-continuous macropores (about 3 μm in size) together with discrete mesopores in the continuous skeletons were identified in all the samples, showing that both the macroscopic and mesoscopic morphologies did not change after surface modification with aminopropyl groups and/or the introduction of Ag NPs (Figure 1). The successful surface modification of silica surface with the aminopropyl groups is confirmed by TG-DTA (Figure S1A) with an explicit exothermic peak between 300 °C and 400 °C on the DTA curve of SiO_2-NH_2 together with the weight loss in the same temperature region on the corresponding TG curve. Such thermal behavior is attributed to the pyrolysis of the aminopropyl groups grafted on the surface of silica. Instead of one-step weight loss, two-step weight loss and their corresponding exothermic behavior, however, were observed in the TG-DTA curves of SiO_2-NH_2-Ag. The weight loss at higher temperature range (250 °C to 400 °C) corresponds to the pyrolysis of aminopropyl groups, while the one observed at lower temperature range (200 °C to 250 °C) could be attributed to decomposition of -$NH_3^+NO_3^-$ ion pairs. A similar result was also observed from the FT-IR measurement (Figure S1B). The spectrum of SiO_2-NH_2-Ag shows a pronounced IR absorption peak at 1385 cm^{-1}, which is commonly observed in the samples containing ionic nitrate [25-27]. After the reduction of Ag^+ by ethanol, HNO_3 as a side product further reacts with the basic -NH_2 groups on the silica surface, which leads to the formation of -$NH_3^+NO_3^-$ ion pairs. The consumption of HNO_3 then further pormotes the reaction to occur towards the reduction of $AgNO_3$ and formation of Ag NPs. The presence of metallic silver in the monolith is confirmed by the XRD pattern of SiO_2-NH_2-Ag (Figure S2). Further atomic information on the surface of the monolith was revealed by XPS measurement. Figure S3 shows the XPS spectrum of SiO_2-NH_2-Ag in the Ag 3d binding energy region. The Ag $3d_{5/2}$ and Ag $3d_{3/2}$ peaks are centered at 367.8 eV and 373.8 eV, respectively, with a spin energy separation of 6.0 eV, which are the characteristics of metallic silver [28]. Peaks corresponding to ionic silver were undetectable in the XPS spectrum of SiO_2-NH_2-Ag. The whole XPS spectrum was shown in the supporting information (Figure S4). The distribution and morphology of Ag NPs embedded in the monolith was observed by TEM (Figure 2). Except for the particles attached on the surface of the macropore skeletons which grows to more than 50 nm

due to the absence of spacial hinderance, most of the Ag NPs are homogeneously located in the mesopores with the average particle size as 2 nm. After surface modification, the aminopropyl groups on the silica skeletons act as the nucleation sites for the growth of Ag NPs. Since most of the surface area is contributed from mesopores and micropores, most of the aminopropyl groups are deduced to be grafted on the surface of meso or micropores. Most of the Ag NPs were therefore grown in these nanometer-sized pores. Although the diffusion-limited parameters for NPs growth became less significant when the reaction time is extended to 14 d, the extremely slow reaction kinetics due to the weak reduction activity of ethanol at room temperature during the reaction process led to the limited growth Ag NPs.

A decrease of adsorbed N_2 volume was observed from N_2 adsorption-desorption isotherms after surface modification with APTES and further immobilization of Ag NPs, giving rise to the reduction of pore volume and BET specific surface area in both the silica used in this research and PMSM (Figure 3 and Table 1). These results are consistent with other results indicating the successful surface modification with aminopropyl groups and the immobilization of Ag NPs thereafter. Average mesopore size remained similar due to big-sized mesopores (24 nm) and small-sized Ag NPs (2 nm) in the mesopores (Figure 2B, Figure 3B and Table 1), which is in accordance with the results from FE-SEM observations (Figure 1D, E, F). However, as PMSM was used as the host silica, due to its periodically aligned cylindrical mesoporous structure and smaller mesopore size, when large amount of Ag NPs was embedded into the mesopores, mesoscale space was easily blocked leading to significant decrease of BET surface area, total pore volume and mesopore size (Figure 3C, D, Table 1).

3.2 Chromatographic separation of aromatic compounds

In our previous report [22], PMSM embedded with Ag NPs showed high potential for the separation of small unsaturated molecules such as polyaromatic hydrocarbons (PAHs), though elution bands with relatively large band broadening and no baseline separation of a mixture of PAHs with different number of aromatic rings was obtained. The improvement of overall separation performance can be expected by the optimization of the pore structure of the host silica monolith as mentioned earlier. The results for the separation of PAHs are shown in Figure 4. Only small differences in retention time among four different compounds (benzene,

naphthalene, anthracene and pyrene) were observed in the cases of SiO_2 and SiO_2-NH_2 monolithic columns as can be seen in Figure 4A and B, possibly due to the differences in size of the compounds. The retention is greatly enhanced when Ag NPs are introduced onto the surface of silica monolith. The elution order is in accordance with the extent of unsaturation in the analyte molecules; the more unsaturated the molecule is, the stronger the interaction between the molecule and Ag NPs is, and the longer the retention time is. Baseline separation of four compounds was achieved with only 25 mg per column loading of Ag in the silica monolith (as compared with 32 mg per column in PMSM), giving the separation factor for anthracene as 0.74 (0.43 for the column of PMSM-NH_2-Ag) and theoretical plate number of 36000 m^{-1} for the retained analyte naphthalene (Table 2). This result clearly indicates that host silica plays a synergic role on the retention behavior and overall separation performance of Ag NPs embedded silica column. Generally reduced plate height is used as a term to compare the intrinsic properties of the porous system for separation and it is given as h = theoretical plate height / skeleton diameter [29,30]. Though the theoretical plate number for retained analyte anthracene is 23000 m^{-1} in SiO_2-NH_2-Ag column, smaller than that of PMSM-NH_2-Ag column (30000 m^{-1}), the h value of SiO_2-NH_2-Ag column is 21.5, much smaller than h = 166.7 in the case of PMSM-NH_2-Ag (the average skeleton diameter as 2 μm and 0.2 μm, respectively for both systems, showing that the SiO_2-NH_2-Ag column is intrinsically much more superior than PMSM-NH_2-Ag for HPLC separation. The increase of mesopore size and change of mesopore shape from cylindrical periodically aligned mesopore to random cylindrical mesopores improve mesopore interconnectivity, which thus accelerates mass transfer in the porous zone making it easier for analyte molecules to access Ag NPs inside the mesopores leading to longer retention time and less band broadening (smaller h value). As a result, with lower Ag NPs loading (25 mg per column), baseline separation of PAHs with higher separation factor (0.74 for analyte anthracene as compared with 0.43 at Ag loading 32 mg per column in PMSM) was achieved. Such results demonstrate the full capability of Ag NPs embedded silica for the separation of PAHs in normal phase mode and the possibility to improve separation performance simply by optimization of the pore structure of host silica.

Stilbenes and their derivatives are commonly found in grapes and other agricultural products. In 1992, epidemiological studies revealed a paradoxical conclusion that polyphenolic components such as phytoalexin

resveratrol in red wine contributes to low incidence of coronary heart disease, known as French paradox [31,32]. Although the detailed mechanism has not yet been totally elucidated, the study of stilbene derivatives, including the effective separation of these compounds, aroused enormous interest among researchers from different research areas [33-37]. Due to the interaction between Ag NPs and unsaturated bonds as has been demonstrated above, there is a high chance that stilbenes and their derivatives can also be separated by Ag NPs embedded silica column. Comparison of separation performance of Ag NPs embedded silica column with pure silica and one modified with aminopropyl groups for *cis* and *trans* stilbene is shown Figure 5. The Ag NPs embedded silica column shows a reasonable baseline separation of *cis* and *trans* isomers of stilbene, while this could not be achieved by pure silica or aminopropyl modified silica columns, which indicates that both silanols and aminopropyl groups on silica surface have weaker interactions with unsaturated bonds than Ag NPs. Retention time for both *cis* and *trans* stilbene is extended with the presence of Ag NPs in silica monolith, presumably due to the Ag^+-like affinity caused by the charge separation on Ag NPs when electron-rich unsaturated aromatic compounds are in contact with Ag NPs [38]. Improved mesoporous structure here ensures better access of analytes to the Ag NPs formed inside the skeletons, which leads to less band broadening and relatively high theoretical plate number. Calculated values of retention factor and theoretical plate number are shown in Table 3. The theoretical plate number for the retained analytes *cis* stilbene and *trans* stilbene are 76000 m^{-1} and 38000 m^{-1}, respectively, and the separation factor is 7, showing much higher separation efficiency for aromatic *cis* and *trans* isomers in the normal-phase mode than that of reported columns (18000 m^{-1} as the theoretical plate number for the retained analyte *cis* stilbene and 1.97 as the separation factor by the HPLC column packed with silica gel modified with poly(octadecyl acrylate) [33] and 3.2 as the separation factor for the HPLC column packed with silica gel modified with poly(acrylonitrile) [34]).

One retention rule that has been established through decades of experiences in silver ion HPLC is that *cis* isomers are always retained stronger than *trans* isomers, due to the relatively stronger charge transfer complexes formed between unsaturated bonds in *cis* isomers and Ag^+ [20]. However, the contradictory result in Figure 5 shows that *trans* stilbene is retained stronger than *cis* stilbene in all the cases, including pure silica

and aminopropyl modified silica as well as Ag NPs embedded silica columns. The geometric difference between *cis* stilbene and *trans* stilbene is considered as the main contributor to the appearance of such elution order. According to the reports by Ihara et al., similar retention order of *cis* and *trans* stilbene isomers was observed from the separation results by silica gels modified with poly(octadecyl acrylate) [33] or poly(acrylonitrile) [34]. Immobilized polymer chains tend to undergo a phase transition between crystal and isotropic states at low temperature. A planar compound such as *trans* stilbene can be easily incorporated with the highly oriented polymer chain while the sterically more bulky *cis* stilbene is geometrically more difficult to interact with the polymer chain, which thus elutes earlier than *trans* stilbene [33]. Similarly crystalline Ag NPs embedded on silica interact with electron-rich molecules as a surface rather than a point in the case of Ag^+. Consequently *trans* stilbene with geometrically more accessible π electrons interacts stronger with Ag NPs leading to a separation at the baseline with a separation factor of 7 for *cis*/*trans* stilbene isomers (Table 3). Such results indicate the high potential of Ag NPs embedded silica column for not only the enhanced separation of unsaturated organic compounds with different unsaturaties but also the recognition of geometrical isomers with the same unsaturaty.

4 Concluding remarks

Ag NPs have been successfully introduced into hierarchically porous silica monolith with optimized porous structure for HPLC separation of unsaturated organic compounds. Baseline separation of PAHs (benzene, naphthalene, anthracene and pyrene) with the theoretical plate number for naphthalene to be 36000 m^{-1} and retention factor for anthracene to be 0.74 was achieved with Ag loading as 25 mg per column. Such enhanced separation performance with less Ag loading (32 mg per column in PMSM) was explained by the better accessibility of analytes to Ag NPs as retention sites in the improved mesopores. Outstanding separation of *cis*/*trans* stilbene isomers with theoretical plate number to be 76000 m^{-1} and 38000 m^{-1}, respectively, and separation factor as 7 was obtained. However the retention of *trans* stilbene was longer than the *cis* isomer which was contradictory to the long established retention rules of Ag^+ HPLC. Such separation behavior was attributed to the more planar molecular geometry of *trans* stilbene, which provides more insights into the detailed separation mechanism of unsaturated compounds by Ag NPs embedded silica column.

Acknowledgements

The present work was financially supported by the Advanced Low Carbon Technology Research and Development Program (ALCA) from the Japan Science and Technology Agency (JST). The authors thank Mr. Wim Smits for fruitful discussion.

The authors have declared no conflict of interest.

References

[1] Kirkland, J. J., *Anal. Chem.* 1965, 37, 1458-1461.

[2] Kirkland, J. J., *Anal. Chem.* 1969, 41, 218-220.

[3] Cintrón, J. M., Colón, L. A., *Analyst* 2002, 127, 701-704.

[4] Chen, L. X., Guan, Y. F., Ma, J. P., Luo, G. A., Liu, K. H., *J. Chromatogr. A* 2005, 1064, 19-24.

[5] Glausch, A., Hirsch, A., Lamparth, I., Schurig, V., *J. Chromatogr. A* 1998, 809, 252-257.

[6] Mitra, S., Karwa, M., *Anal. Chem.* 2006, 78, 2064-2070.

[7] Moliner-Martínez, Y., Ribera, A., Coronado, E., Campíns-Falcó, P., *J. Chromatogr. A* 2011, 1218, 2276-2283.

[8] Krenkova, J., Foret, F., *J. Sep. Sci.* 2011, 34, 2106-2112.

[9] Arrua, D., Haddad, P. R., Hilder, E. F., *J. Chromatogr. A* 2013, 1311, 121-126.

[10] Arrua, D., Nordborg, A., Haddad, P. R., Hilder, E. F., *J. Chromatogr. A* 2013, 1273, 26-33.

[11] Krenkova, J., Lacher, N., A., Svec, F., *Anal. Chem.* 2010, 82, 8335-8341.

[12] Nilsson, C., Nilsson, S., *Electrophoresis* 2006, 27, 76-83.

[13] Nilsson, C., Viberg, P., Spégel, P., Jörntén-Karlsson, M., Peterson, P., Nilsson, S., *Anal. Chem.* 2006, 78, 6088-6095.

[14] Zhang, Z. X., Yan, B., Liao, Y. P., Liu, H. W., *Anal. Bioanal. Chem.* 2008, 391, 925-927.

[15] Yang, L., Guihen, E., Holmes, J. D., Loughran, M., O'Sullivan, G. P., Glennon, J. D., *Anal. Chem.* 2005, 77, 1840-1846.

[16] Xu, Y., Cao, Q., Svec, F., Frechet, J. M. J., *Anal. Chem.* 2010, 82, 3352-3358.

[17] Lv, Y., Lin, Z., Svec, F., *Anal. Chem.* 2012, 84, 8457-8460.

[18] Liang, X., Wang, X., Ren, H., Jiang, S., Wang, L., Liu, S., *J. Sep. Sci.* 2014, 37, 1371-1379.

[19] Morris, L. J., *J. Lipid Res.* 1966, 7, 717-732.

[20] Nikolova-Damyanova, B., *J. Chromatogr. A* 2009, 1216, 1815-1824.

[21] Sedlacek, O., Kucka, J., Svec, F., Hruby, M., *J. Sep. Sci.* 2014, 37, 798-802.

[22] Zhu, Y., Morisato, K., Li, W., Kanamori, K., Nakanishi, K., *ACS Appl. Mater. Interfaces* 2013, 5, 2118-2125.

[23] Poppe, H., *J. Chromatogr. A*, 2002, 948, 3-17.

[24] Nakanishi, K., Shikata, H., Ishizuka, N., Koheiya, N., Soga, N., *J. High Resol. Chromatogr.* 2000, 23, 106-110.

[25] Qian, J. M., Jin, Z. H., *J Eur. Ceram. Soc.* 2006, 26, 1311-1316.

[26] Nakamoto, K., *Infrared and Raman Spectra of Inorganic and Coordination Compounds*, 6th ed.; Wiley-Interscience: New York, 2009.

[27] Linker, R., Shmulevich, I., Kenny, A., Shaviv, A., *Chemosphere* 2005, 61, 652-658.

[28] Moulder, J. F., Stickle, W. F., Sobol, P. E., Bomben, K. D., *Handbook of X-ray Photoelectron Spectroscopy*, (Ed.: Chastain, J.), Perkin-Elmer Corporation, USA, 1992, pp. 182.

[29] Giddings, J. C., *J. Chromatogr. A* 1964, 13, 301-304.

[30] Vervoort, N., Gzil, P., Baron, G. V., Desmet, G., *J. Chromatogr. A* 2004, 1030, 177-186.

[31] Renaud, S., Lorgeril, M. de, *Lancet* 1992, 339, 1523-1526.

[32] Hain, R., Reif, H-J., Langebartels, R., Kindl, H., Vornam, B., Wiese, W., Schmelzer, E., Schreier, P. H., Stöcker, R. H., Stenzel, K., *Nature* 1993, 361, 153-156.

[33] Fukumoto, T., Ihara, H., Sakaki, S., Shosenji, H., Hirayama, C., *J. Chromatogr. A* 1994, 672, 237-241.

[34] Ihara, H., Okazaki, S., Ohmori, K., Uemura, S., Hirayama, C., Nagaoka, S., *Anal. Sci.* 1998, 14, 349-354.

[35] Goldberg, D. M., Ng, E., Karumanchiri, A., Yan, J., Diamandis, E. P., Soleas, G. J., *J. Chromatogr. A* 1995, 708, 89-98.

[36] Baptista, J. A. B., Tavares, J. F. da P., Carvalho, R. C. B., *Food Res. Int.*, 2001, 34, 345-355.

[37] Király-Véghely, Z., Kátay, G., Tyihák, E., Merillon, J., *J. Planar Chromatogr.*, 2004, 17, 5-8.

[38] Pozun, Z. D., Tran, K., Shi, A., Smith, R. H., Henkelman, G., *J. Phys. Chem. C*, 2011, 115, 1811-1818.

Table 1 Pore characteristics of the monoliths SiO_2, SiO_2-NH_2, SiO_2-NH_2-Ag and PMSM, PMSM-NH_2, PMSM-NH_2-Ag for column preparation calculated from N_2 adsorption desorption isotherms.

Sample	S_{BET} ($m^2 g^{-1}$)	[b]S_{BET} in column (m^2)	V_p ($cm^3 g^{-1}$)	D_p (nm)
SiO_2	230	85	0.94	24.4
SiO_2-NH_2	180	74	0.77	21.3
SiO_2-NH_2-Ag	160	72	0.69	24.4
[a]PMSM	380	53	0.81	9.2
PMSM-NH_2	310	50	0.68	8.1
PMSM-NH_2-Ag	140	29	0.29	7.1

[a] PMSM was calcined at 800 °C while the rest of the monoliths were calcined at 600 °C.

[b] monoliths for column preparation are all in cylinder shape (83 mm in length and 4.6 mm in diameter) with their weight to be 0.37 g, 0.41 g, 0.45 g and 0.14 g, 0.16 g, 0.21 g for SiO_2, SiO_2-NH_2, SiO_2-NH_2-Ag and PMSM, PMSM-NH_2, PMSM-NH_2-Ag, respectively.

Table 2 Calculated values of retention factor, theoretical plate number for aromatic hydrocarbons separated by SiO_2-NH_2-Ag monolithic column.

	[a]k	[b]N (m)
Benzene	0	33000
Naphthalene	0.20	36000
Anthracene	0.74	23000
Pyrene	1.1	21000

[a] Retention factor calculated as $(t - t_b) / t_b$, where t is the elution time of naphthalene, anthracene or pyrene and t_b is the elution time of benzene (due to the lack of proper t_0 sample).

[b] Theoretical plate number calculated as 5.54 $(t / w_{0.5})$, where t and $w_{0.5}$ are the retention time and band width at half height.

Table 3 Calculated values of retention factor, theoretical plate number for *cis*- and *trans*-stilbene separated by SiO2-NH2-Ag monolithic column.

	k	***N* (m)**	[a]***α***
cis-stilbene	0.05	76000	7
trans-stilbene	0.35	38000	

[a] Separation factor calculated as k_t/k_c, where k_t and k_c are the retention factors of *trans*-stilbene and *cis*-stilbene.

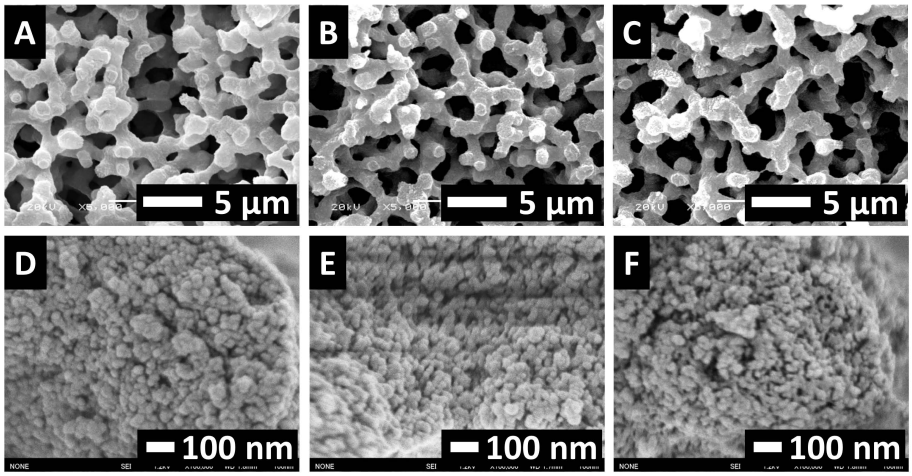

Figure 1 SEM and FE-SEM images of the monoliths: SiO_2 (A, D), SiO_2-NH_2 (B, E) and SiO_2-NH_2-Ag (C, F).

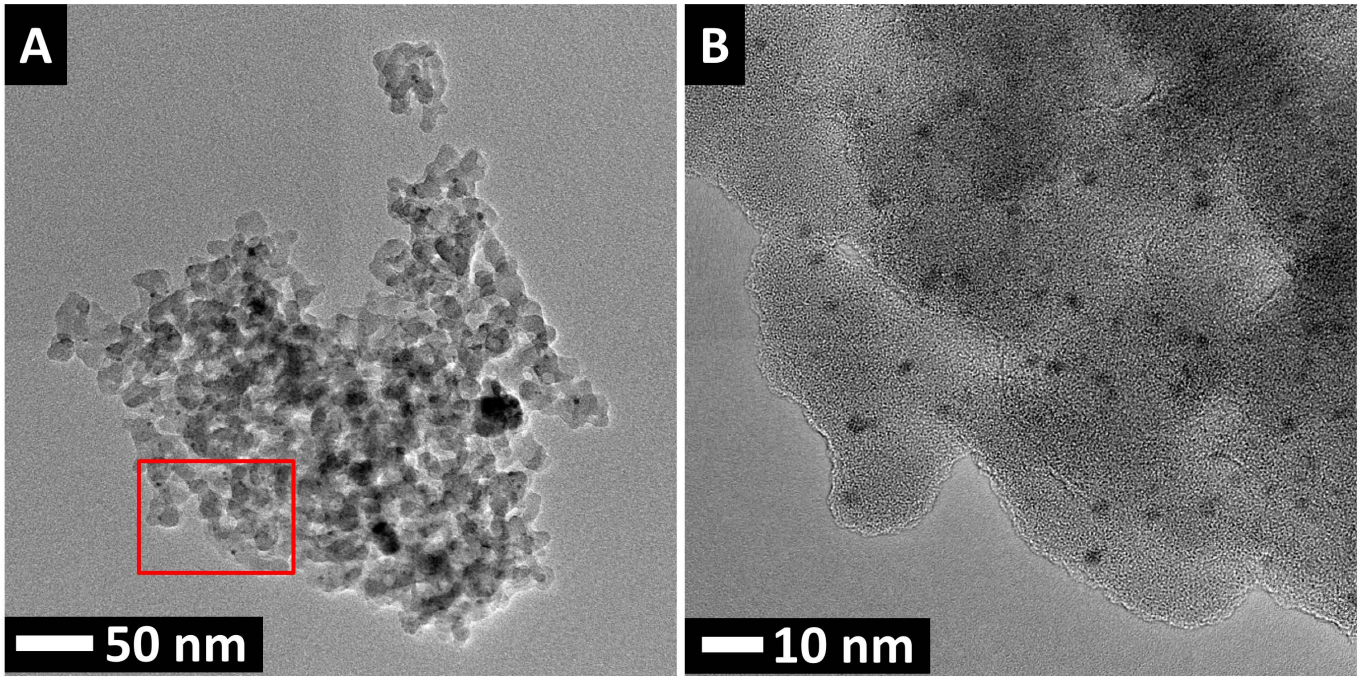

Figure 2 TEM image of SiO_2-NH_2-Ag (A) and the magnified image at the part pointed out by the red frame (B).

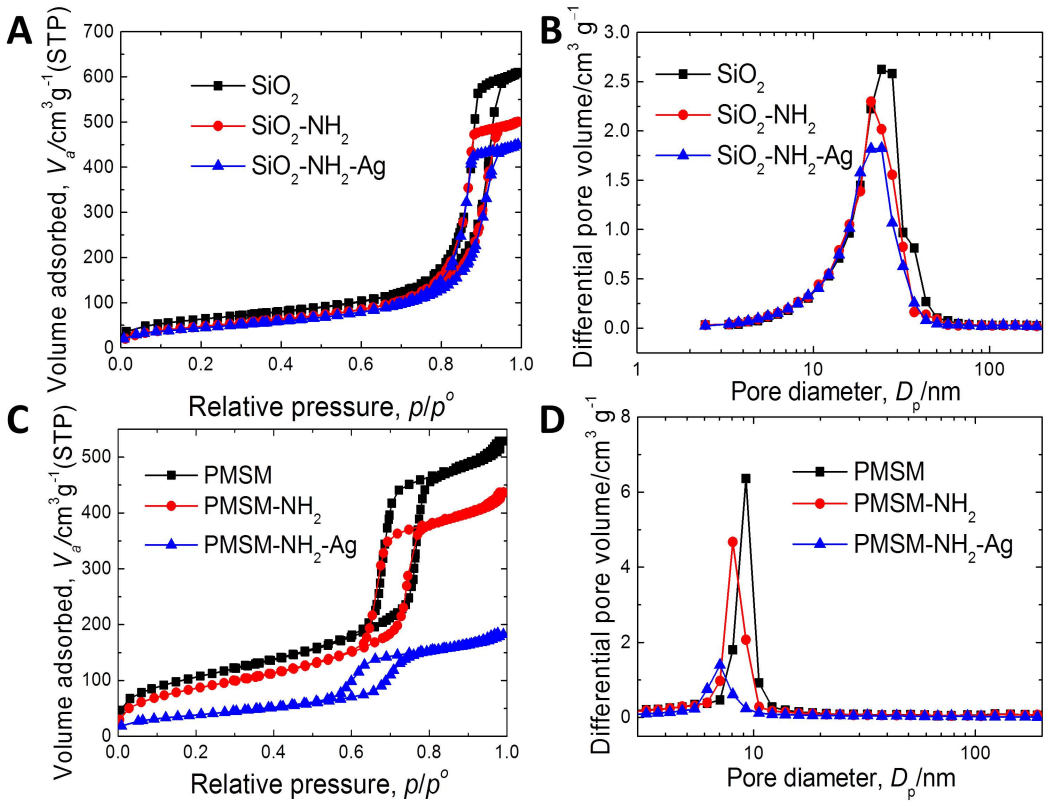

Figure 3 Nitrogen adsorption desorption isotherms and BJH pore size distributions calculated from the adsorption branch of the monoliths SiO_2, SiO_2-NH_2, SiO_2-NH_2-Ag (A, B) and PMSM, PMSM-NH_2, PMSM-NH_2-Ag (C, D).

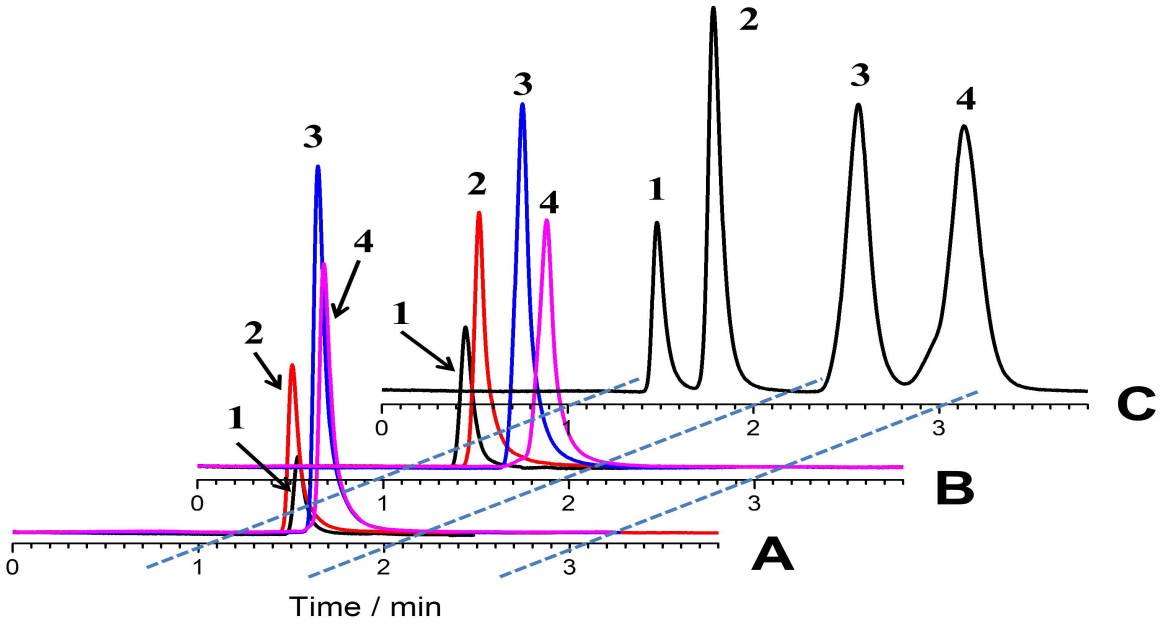

Figure 4 Chromatograms of benzene (1), naphthalene (2), anthracene (3) and pyrene (4), using monolithic SiO_2 (A), SiO_2-NH_2 (B) and SiO_2-NH_2-Ag (C) columns. Conditions: mobile phase 0.2% acetonitrile / hexane, flow rate 1.0 mL/min, detector UV254 nm, pressure 2.1 MPa, column length 83 mm, temperature 25 ℃.

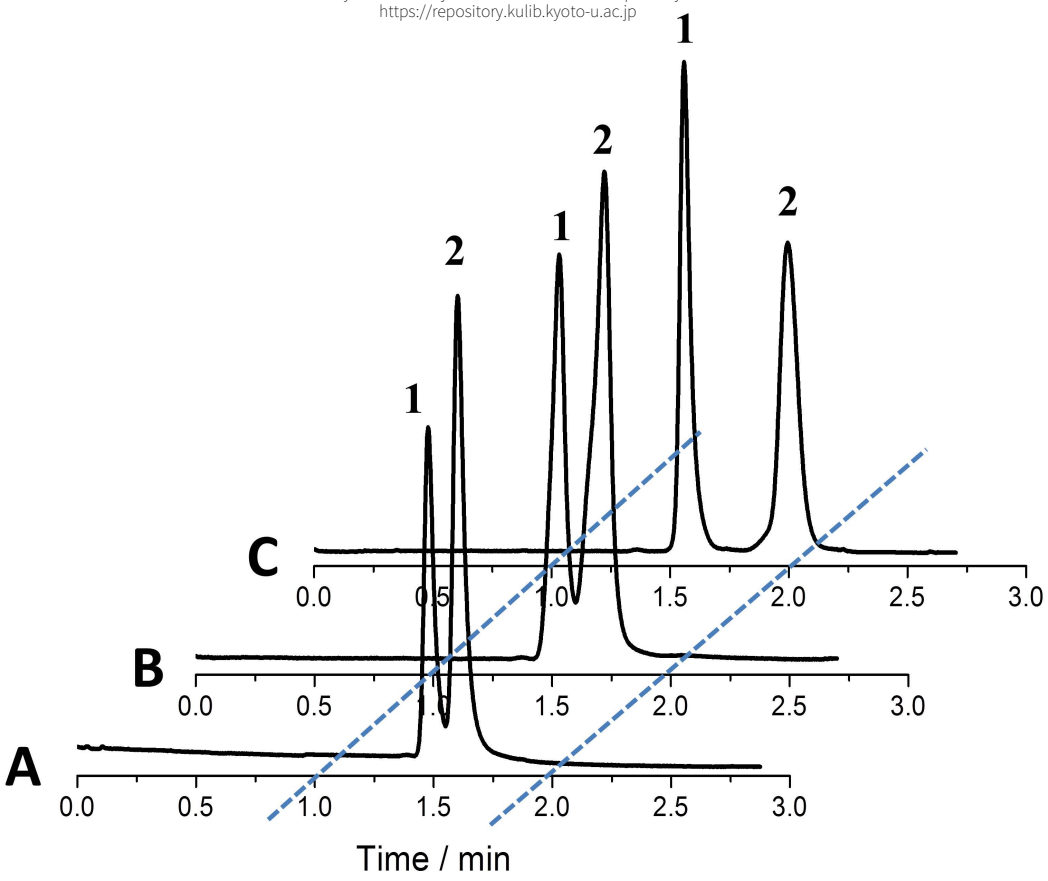

Figure 5 Chromatograms of *cis*-stilbene (1) and *trans*-stilbene (2), using monolithic SiO_2 (A), SiO_2-NH_2 (B) and SiO_2-NH_2-Ag (C) columns. Conditions: mobile phase 0.2% acetonitrile / hexane, flow rate 1.0 mL/min, detector UV254 nm, pressure1.5 MPa, column length 83 mm, and temperature 25 ℃.

HPLC Separation of Unsaturated Organic Compounds by Ag NPs embedded Silica Column

Yang Zhu[1], Kei Morisato[2], George Hasegawa[1], Nirmalya Moitra[1], Tsutomu Kiyomura[3], Hiroki Kurata[3], Kazuyoshi Kanamori[1], Kazuki Nakanishi[1]

[1] Department of Chemistry, Graduate School of Science, Kyoto University, Kitashirakawa, Sakyo-ku, Kyoto 606-8502, Japan

[2] GL Science, Inc. 237-2 Sayamagahara, Iruma, Saitama, 358-0032, Japan

[3] Institute for Chemical Research, Kyoto University, Uji, 611-0011, Japan

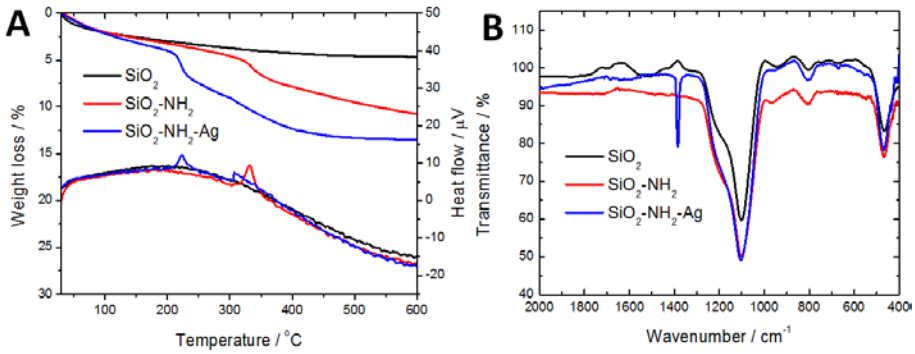

Figure S1 TG-DTA curves (A) and FT-IR spectra (B) and of monoliths: SiO_2, SiO_2-NH_2, SiO_2-NH_2-Ag.

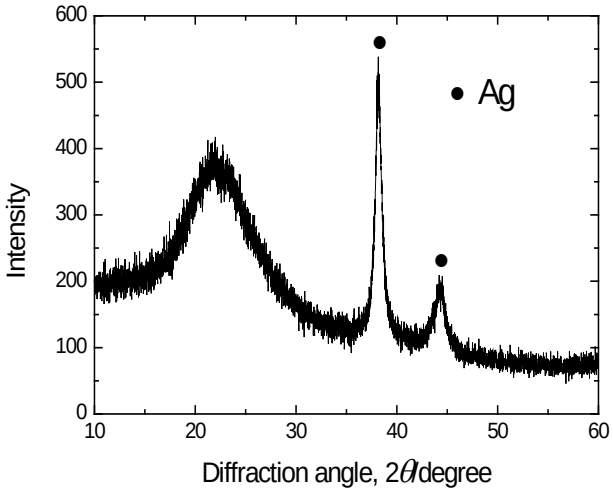

Figure S2 XRD pattern of SiO_2-NH_2-Ag.

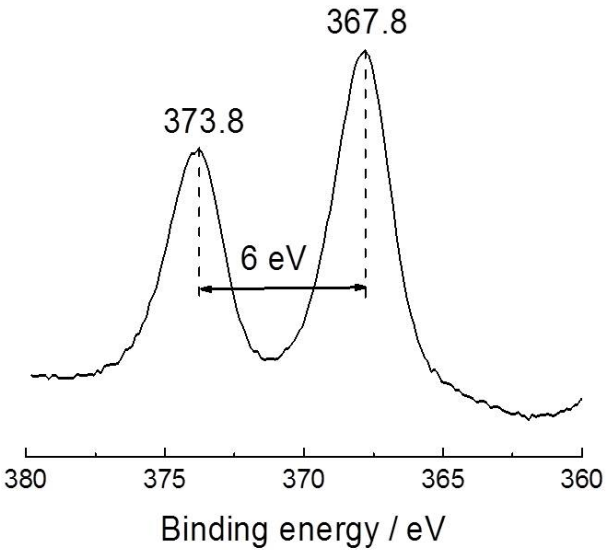

Figure S3 XPS spectrum of Ag 3d for SiO_2-NH_2-Ag.

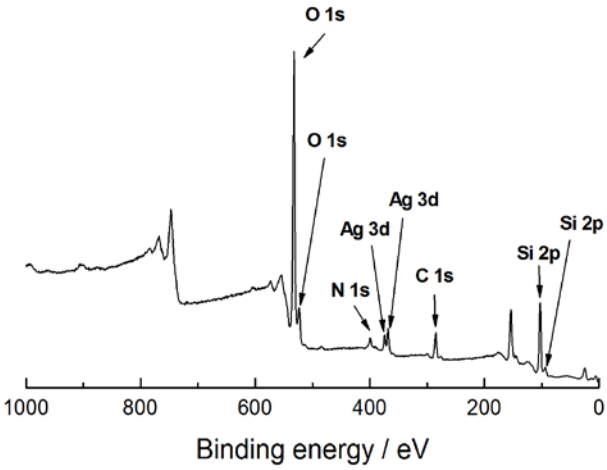

Figure S4 Full XPS spectrum of monolith: SiO_2-NH_2-Ag.